

Elsevier Editorial System(tm) for  
Microporous & Mesoporous Materials  
Manuscript Draft

Manuscript Number: MICMAT-D-17-01003R1

Title: Dehydration mechanism of AlPO<sub>4</sub>-5: a high-resolution synchrotron X-ray powder diffraction study

Article Type: Full length article

Keywords: AlPO<sub>4</sub>-5, High temperature XRPD, dehydration, negative thermal expansion

Corresponding Author: Dr. Rossella Arletti,

Corresponding Author's Institution: University of Turin

First Author: Michelangelo Polisi

Order of Authors: Michelangelo Polisi; Rossella Arletti; Simona Quartieri; Linda Pastero; Carlotta Giacobbe; Giovanna Vezzalini

Abstract: We present the results of a study on the thermal stability and dehydration dynamics of the porous aluminophosphate AlPO<sub>4</sub>-5, from room temperature to 850 °C, carried out by in situ synchrotron X-ray powder diffraction experiments. No phase transitions were observed in the investigated T range. Due to the very low interactions among framework and water molecules, dehydration is already complete at 152 °C. It occurs in two main T ranges, one between 60 and 80 °C and the second one between 90 and 120 °C. During these two stages, the cell volume tends to increase to facilitate the water release. Overall, across the full explored T range, the cell volume increase is only 0.84%, indicating that AlPO<sub>4</sub>-5 is one of the most rigid zeolite frameworks studied to date. Specifically, after complete dehydration at 200 °C, AlPO<sub>4</sub>-5 undergoes a negative thermal expansion as a consequence of the decrease in both a and c cell parameters. The expansion coefficients for V, a and c cell parameters, in the 152-850 °C range, are  $\alpha_V = -7.12$  (10<sup>-6</sup>/K),  $\alpha_a = -2.5$  (10<sup>-6</sup>/K),  $\alpha_c = -2.2$  (10<sup>-6</sup>/K), respectively.



UNIVERSITÀ DEGLI STUDI DI TORINO  
**DIPARTIMENTO DI SCIENZE DELLA TERRA**  
 Via Valperga Caluso, 35 - 10125 TORINO – Italy



**Prof. Rossella Arletti**

[rossella.arletti@unito.it](mailto:rossella.arletti@unito.it)

Phone: +39.011.6705129

Fax: +39.011.6705128

Torino, October 3<sup>rd</sup> 2017

Dear Editor,

please find enclosed the revised version of the manuscript "Dehydration mechanism of AIPO<sub>4-5</sub>: a high-resolution synchrotron X-ray powder diffraction study" by Polisi et al., modified according to the reviewer's comments. The anonymous referees are acknowledged for their contributions, that helped us in improving the manuscript. We hope that now it is suitable for publication in MMM.

Best regards

On behalf of the co-authors

Rossella Arletti

Reviewer #1:

The authors provided a technically sound study on the dehydration behavior of AIPO<sub>4-5</sub>. Structural changes of the AIPO<sub>4</sub> during thermal dehydration have been investigated in-situ by synchrotron radiation experiments. The work fits into the scope of MICMAT and the manuscript is well written. I think one point needs some more attention. In the introduction the authors report that similar studies have been performed before, with the major difference that the present paper provides details of structural changes during NTE and dehydration. Since this is supposed to be the point where novelty can be claimed, I was surprised that the respective section in the manuscript elaborates phenomenologically on different observations but a clear explanation what is going on during these processes is not provided. After reading the complete manuscript I am still not aware of which physical or structural effect causes the NTE nor why a and c axes experience a decrease upon dehydration below 100°C. In my opinion, the structural changes going along with the dehydration and NTE need to be discussed in way more detail, otherwise the content of new information would be only moderate and I would doubt that a more or less phenomenological description of results would grant publication in MICMAT. However, I am sure that the authors can expand the respective section and provide valuable insights into the interaction of water and the AIPO<sub>4</sub> framework

*After the comment of the referee the structural interpretation of the phenomena was deeply improved. Specifically, the structural modifications occurring during the water migration and release were understood and discussed. Concerning the NTE, we did not detail further this section being the phenomenon very limited in the T range 150°C-850°C ( $\Delta V = -0.5\%$ ;  $\Delta a = -0.2\%$  and  $\Delta c = -0.1\%$ )*

- Axis labels and text are too small to be readable in many figures, especially not if they get reduced in size in the printed version of the journal.

*The Figures were improved and now are more readable.*

- Figure 2 is of relatively poor quality and I recommend replacement by a figure of better quality that

allows to see details of changes of the XRD patterns. If the latter cannot be seen, the figure is of little to no use.

*We improved the resolution of the figure and maintained it in the new Supplementary Information. In our opinion, it clearly shows the crystallinity preservation. Moreover, the change in the peak intensities clearly reflects the dehydration dynamics.*

- AlPO<sub>4</sub>-5 growth as elongated hexagonal prisms, likely causing preferred orientation effects in the XRD patterns. The authors did not explain how they handled these (grinding of the samples? Refinement/consideration of preferred orientation in GSAS? ...)

*The sample was ground before the analyses ( this was added in the experimental section).*

*We checked the refinements and, from the refinement there was no sign of preferred orientations.*

- It would be interesting to see SEM or optical microscopy images of the AlPO<sub>4</sub>-5 sample used for the study.

*The picture was added*

- How do authors explain the fact that U(iso) is larger at lower temperatures than at higher ones - this is counter-intuitive, isn't it?

*The decrease of U<sub>iso</sub> upon heating mainly involves the framework atoms. This could be the effect of a slight ordering increase favored by temperature. In fact, it is largely reported that at rT AlPO<sub>4</sub>-5 is characterized by high disorder – leading high and strongly anisotropic thermal parameters, especially on the framework oxygen atoms. This point is cited in the Introduction.*

- The authors write "Corresponding with these two stages, the cell volume tends to increase to facilitate water release." In my opinion, the elevated temperature facilitates the release of water and not so much the relatively moderate increase of pore sizes.

*The mechanism of water release and the "breathing" of the rings is now well explained in the manuscript*

## Reviewer #2:

-All over the manuscript: physical variables such as temperature (T), volume (V) unit-cell axes (a and c) should be reported in italic.

-Abstract, line 7: I would replace "complete T range" with "full T range"

-Abstract lines 11-12: the authors should state explicitly that the reported expansion coefficients refer to the 152-850 °C range

-Introduction, line 2: replace "several applications" with "various applications" or something similar ("several" is already reported in the previous line)

-Introduction, page 2, line 16: thermal expansion coefficients

-Introduction, page 2, line 18: material -> compound

-Introduction, page 2, line 19:  $[\alpha]V = -14.5(4.6) \cdot (10^{-6}/K)$  (10<sup>-6</sup>/K is missing)

-Section 2, page 2, line 2 and all over the manuscript: in the space group notations the numbers should not be reported in italic

-Page 3, section 3.1, line 6: in the gel composition remove the spaces after the colons (:), or add spaces before them.

-Page 4, section 3.3, line 7: I would replace "under 92°C" with "below 92 °C"

-Page 4, section 3.3, lines 7-10: there's clearly something missing here -> patterns were collected every 10 °C below 92 °C and in the 122-152 °C range, then every 5 °C in the 92-122 °C range (and that range

in missing).

-Page 4, section 3.4, lines 6 and 17: add a space between the temperature and °C

-Page 5, section 4.1, line 2: I think that "p.u.c." should be defined the first time as standing for "per unit cell"

-Page 5, section 4.2.1, line 10: as before I would replace "under" with "below"

-Page 6, section 4.2.2, line 5: 2.56 Å (Å is missing)

*-All these correction were reported in the revised version*

-Page 6, section 4.2.2, lines 5-8: "The difference in water contents estimated from the refinement and from the TG analyses are due to the presence of superficial water and, possibly, different times at which TG analysis and XRPD collection were performed". Surface water and different starting hydration of the zeolite are surely possible reasons for the different water content determined from TG and structure refinement. However, a further (likely) possible reason is due to the restraints applied to the displacement parameters of the water sites during the refinement: i.e. one isotropic parameter for all the sites. These restraints are necessary for a stable refinement, but may significantly bias the refined values of the occupancy factors and, therefore, the estimated absolute value of the water molecules. This does not affect significantly the discussion on the dehydration mechanism (as this is substantially normalized to the room-T refinement and also based on the difference-Fourier maps of the electron density), but makes difficult a comparison among the estimated water content from the refinement and the TG analysis.

*From the TG analyses it was demonstrated that the dehydrated sample progressively rehydrates once it is in contact with air (from 7.6 to 16.5 water molecules per unit cell). So the most probable hypothesis for the difference in the estimated water contents is a different degree of hydration of the sample exposed to air. The progressive rehydration of the sample is now better explained in the text. Anyway, tests on the influence of  $U_{iso}$  on the occupancy factors of water molecules were performed. We observed expected effects on the occupancy factors, but not so high to justify these differences.*

-Page 6, section 4.2.2, lines 24-25: "corresponding to 0.48 molecules" I would report that this is per unit cell

*Text was corrected*

-Page 6, section 4.2.2, line 29: replace Figure 6b with 5b

*Text was corrected*

-Page 7, section 4.2.3, line 5: replace O1-O4 ring with O1-O4 diameter

*Text was corrected*

-Page 7, section 4.2.3, lines 15-17: "As reported by [18] this large value, even at rT, actually derives from the coexistence of three domains in the structure of AlPO<sub>4</sub>-5. The result is an average position of the O<sub>2</sub> atom, causing the very high thermal displacement parameters of this oxygen, as discussed above". This is only one of the hypotheses reported in the literature for explaining the positional disorder of the framework oxygen sites along specific directions. As the authors report in section 2 (page 3) the presence of dynamic rigid unit modes of tilting of the tetrahedra was also suggested for zeolite AlPO<sub>4</sub>-5

*This section has been removed in the new manuscript version*

-Page 8, section 4.2.4, line 10-11: 5 °C/h, min (C is missing)

*Text was corrected*

-Table 1 caption: Experimental and statistical (?) parameters

-Table 1S, T = 152: b should be 8.42480(4)

-Tables 2S: I would remove the esd = 0 from the fractional coordinates constrained by symmetry

*Text was corrected*



UNIVERSITÀ DEGLI STUDI DI TORINO  
DIPARTIMENTO DI SCIENZE DELLA TERRA  
Via Valperga Caluso, 35 - 10125 TORINO – Italy



**Prof. Rossella Arletti**

[rossella.arletti@unito.it](mailto:rossella.arletti@unito.it)

Phone: +39.011.6705129

Fax: +39.011.6705128

---

Torino, July 07, 2017

In the following, we provide a list of colleagues who could comment and review our work:

Prof. Annalisa Martucci, Dipartimento di Fisica e Scienze della Terra, University of Ferrara, Italy

[annalisa.martucci@unife.it](mailto:annalisa.martucci@unife.it)

Dr. Julien Haines, Institut Charles Gerhardt, Montpellier, France

[julien.haines@univ-montp2.fr](mailto:julien.haines@univ-montp2.fr)

Dr. Martin Fisch, Institute of Geological Sciences, Universität Bern, Switzerland

[martin.fisch@geo.unibe.ch](mailto:martin.fisch@geo.unibe.ch)

Dr. Paolo Lotti, Dipartimento di Scienze della Terra, University of Milan, Italy

[paolo.lotti@unimi.it](mailto:paolo.lotti@unimi.it)

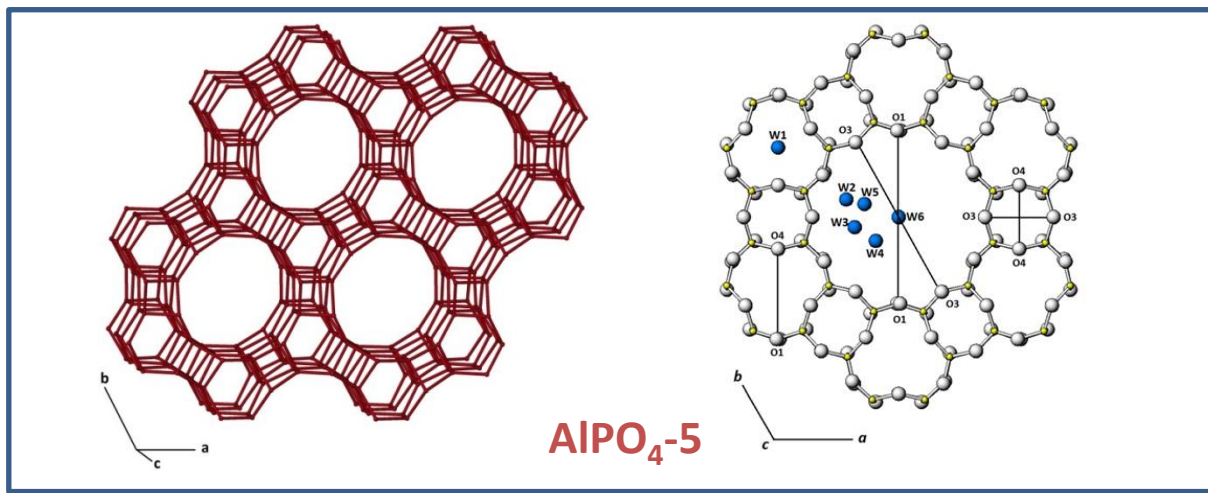
We shall be glad to give you any additional information you would need.

With very best regards, yours sincerely,

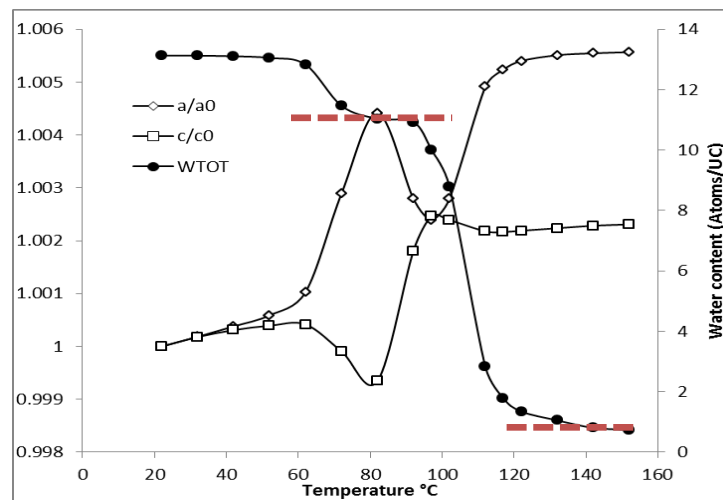
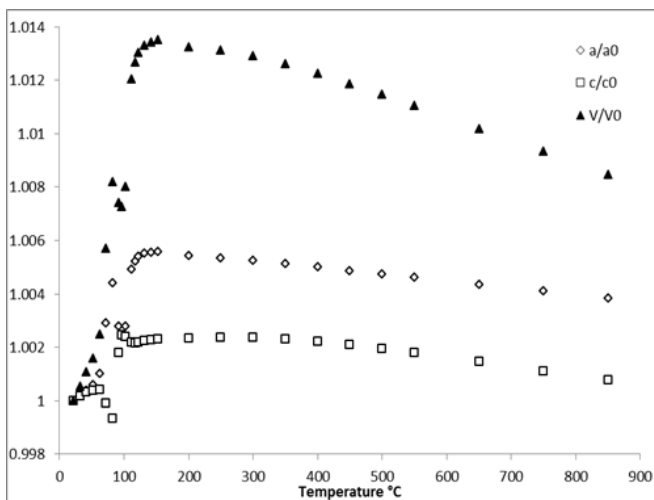
Rossella ARLETTI

On behalf of the co-authors

- In situ synchrotron XRPD study of  $\text{AlPO}_4\text{-5}$  dehydration dynamic from rT to 850 °C
- No phase transitions were observed in the investigated T range.
- After complete dehydration (at 152 °C)  $\text{AlPO}_4\text{-5}$  undergoes a negative thermal expansion
- In the ranges 60-80 and 90-120°C, the cell V increases to facilitate water release
- $\text{AlPO}_4\text{-5}$  is one of the most rigid zeolites studied to date ( $\Delta V=0.84\%$  from rT to 850 °C)



**HT**



**Dehydration mechanism of AlPO<sub>4</sub>-5:  
a high-resolution synchrotron X-ray powder diffraction study**

Michelangelo Polisi<sup>a</sup>, Rossella Arletti<sup>b</sup>, Simona Quartieri<sup>c</sup>, Linda Pastero<sup>b</sup>,  
Carlotta Giacobbe<sup>d</sup>, Giovanna Vezzalini<sup>a</sup>

<sup>a</sup> *Dipartimento di Scienze Chimiche e Geologiche, Università di Modena e Reggio Emilia, via  
Campi 103, I- 41125 Modena, Italy*

<sup>b</sup> *Dipartimento di Scienze della Terra, Università di Torino, Via Valperga Caluso 35, I-10125  
Torino, Italy.*

<sup>c</sup> *Dipartimento di Scienze Matematiche e Informatiche, Scienze Fisiche e Scienze della Terra,  
Università di Messina, viale F. Stagno d'Alcontres 31, I-98166 Messina S. Agata, Italy.*

<sup>d</sup> *ESRF, F-3800 Grenoble, France*

## Abstract

We present the results of a study on the thermal stability and dehydration dynamics of the porous aluminophosphate AlPO<sub>4</sub>-5, from room temperature to 850 °C, carried out by in situ synchrotron X-ray powder diffraction experiments. No phase transitions were observed in the investigated  $T$  range. Due to the very low interactions among framework and water molecules, dehydration is already complete at 152 °C. It occurs in two main  $T$  ranges, one between 60 and 80 °C and the second one between 90 and 120 °C. During these two stages, the cell volume tends to increase to facilitate the water release. Overall, across the full explored  $T$  range, the cell volume increase is only 0.84%, indicating that AlPO<sub>4</sub>-5 is one of the most rigid zeolite frameworks studied to date. Specifically, after complete dehydration at 200 °C, AlPO<sub>4</sub>-5 undergoes a negative thermal expansion as a consequence of the decrease in both  $a$  and  $c$  cell parameters. The expansion coefficients for  $V$ ,  $a$  and  $c$  cell parameters, in the 152-850 °C range, are  $\alpha_V = -7.12$  ( $10^{-6}/\text{K}$ ),  $\alpha_a = -2.5$  ( $10^{-6}/\text{K}$ ),  $\alpha_c = -2.2$  ( $10^{-6}/\text{K}$ ), respectively.

## Keywords

AlPO<sub>4</sub>-5, High temperature XRPD, dehydration, negative thermal expansion

## 1. Introduction



Aluminophosphates [1,2] are a group of microporous materials sharing several framework types with zeolites [2,3], with various applications as molecular sieves, catalysts, etc. [1].

One member of this family, AlPO<sub>4-5</sub> [4] (AFI-framework type [5]) has become the object of increasing interest thanks to its potential technological and industrial applications [6,7,8]. AFI-framework is characterized by a monodimensional channel system defined by 12-membered tetrahedral rings (12MR) (Figure 1), suitable for hosting organic molecules and polymers. In particular, the regular nanometric channel system exhibited by AlPO<sub>4-5</sub> makes this porous material an ideal matrix for achieving supramolecular organization, making it possible to obtain hierarchically organized multifunctional composite materials [9,10,11]. These materials are in general synthesized after a high temperature treatment, to free up space in the channel system by water release. Since the successful synthesis and properties of these hybrid systems crucially depend on the pore dimensions, it is essential to obtain information on the thermal stability of AlPO<sub>4-5</sub> upon calcination and on its possible framework deformations.

While the elastic behavior of AlPO<sub>4-5</sub> has been studied, even very recently, by a number of authors [12,13,14], data on dehydration and thermal behavior are very limited. Park et al. [15], studying the thermal expansion coefficients of some microporous materials, investigated AlPO<sub>4-5</sub> in the  $T$  range 298-774 K, using the X-ray diffraction Lenné-Guinier technique. In the first heating stages, the compound exhibited positive volume expansion, while at high  $T$  it contracted upon heating, with a negative thermal expansion (NTE) coefficient  $\alpha_v = -14.5(4.6) (10^{-6})/\text{K}$ . However, the paper does not report neither structural data nor interpretation of the modifications during dehydration process.

The present study aims to obtain more detailed information on the thermal behavior of AlPO<sub>4-5</sub>, deriving the  $T$ -dependence of unit cell parameters, water migration and crystal structure, on the basis of in situ synchrotron X-ray powder diffraction (XRPD) experiments performed from room  $T$  ( $rT$ ) to 850 °C.

## 2. AFI zeolite structure

The synthetic AlPO<sub>4-5</sub> aluminophosphate exhibits topological symmetry  $P6/mcc$  and cell parameters  $a = b = 13.827 \text{ \AA}$ , and  $c = 8.580 \text{ \AA}$ . The framework (Figure 1) is characterized by 12-membered ring (12MR) channels parallel to the [001] direction, with a free diameter of 7.3 Å. The channels are connected each other by “pseudo-cage” cavities which are confined in the (001) plane by a single six-membered ring (6MR) of tetrahedra centered on the 3-fold axis.

The alternating distribution of Al and P in the tetrahedra reduces the symmetry of  $\text{AlPO}_4\text{-5}$  from the topological  $P6/mcc$  to a lower one. Conflicting results are reported in literature concerning the real symmetry of  $\text{AlPO}_4\text{-5}$ . Several authors (see [16] for a review) noticed large anisotropic displacement parameters for the oxygen atoms and an almost linear Al-O2-P bond angle in the structure refinements. On the basis of these data, different lower symmetries were proposed, among which: 1) Mora et al. [17] suggested a symmetry reduction to the orthorhombic subgroup  $Pcc2$ ; 2) Klap et al. [18] proposed an average  $P6cc$  structure deriving by the presence of three co-existing structural micro-domains with local symmetry  $P6$ ; 3) other authors [19,20] discussed the presence of diffuse scattering along specific directions parallel to the  $c^*$  axis and on the (001) plane, and proposed that this effect is related to the presence of different rigid unit modes (RUMs) of structure deformation, i.e. specific modes of tilting of the tetrahedra, which lead to a dynamic disorder of the framework atoms; 4) finally, in a recent single-crystal diffraction study, an incommensurately modulated structure, with a modulation vector of  $0.37c$ , was observed [14].

These literature data clearly demonstrate that the structural refinement of this porous phase is not trivial. For our structural study we adopted the s.g.  $P6cc$ .

### 3. Experimental section

#### 3.1 Materials

The  $\text{AlPO}_4\text{-5}$  sample used in this work was obtained by modifying the synthesis routine proposed by Liu et al. [21] as follows. Firstly, 4.1 g of aluminum isopropoxide was hydrolyzed for 4 h, under magnetic stirring, in 18 ml of ultrapure water obtained using an Elga Flex3 water purification system. 3 g of phosphoric acid (85%) were added and the suspension was stirred further for 1 h. Finally, 0.835 ml of triethylamine template (TEA) was added under no stirring, and then stirred for 10 min. The molar composition of the synthesis gel was:  $1\text{Al}_2\text{O}_3:1.33\text{P}_2\text{O}_5:0.6\text{TEA}:102.5\text{H}_2\text{O}$ . A secondary electron image of one synthesized crystal is reported in Figure 2.

The precursor gel was kept at  $rT$  for 12 h and then transferred into a Teflon-lined autoclave and heated at  $210\text{ }^\circ\text{C}$  for 4 days. In order to remove the organic template TEA from the zeolite cavities, the as-synthesized sample was calcined at  $600\text{ }^\circ\text{C}$ .

#### 3.2 Thermogravimetric analyses

TG analyses of calcined  $\text{AlPO}_4\text{-5}$  crystals were carried out using a Seiko SSC/5200 thermal analyzer under the following experimental conditions: the sample was loaded into a Pt crucible and heated in the temperature range  $rT\text{-}1050\text{ }^\circ\text{C}$ ; the heating rate was  $10\text{ }^\circ\text{C}/\text{min}$  with an air flux of 100

$\mu\text{L}/\text{min}$ . Two different TG analyses were performed on the same sample, one a few days after the calcination process (TG1) and another several months after (TG2) (Figure 3).

### 3.3 XRPD data collection

The temperature-resolved XRPD data were collected at ID22 beamline at ESRF (Grenoble, France) with a fixed wavelength of  $0.3999 \text{ \AA}$ . The powder sample was grinded and then loaded and packed into a  $0.3 \text{ mm}$  quartz capillary. The capillary was mounted on a standard goniometric head and kept spinning during pattern collection. The sample was heated *in-situ* using a hot-air blower from  $rT$  to  $850 \text{ }^\circ\text{C}$  with a heating rate of  $5 \text{ }^\circ\text{C}/\text{min}$ . The diffraction patterns were recorded with a high-resolution multianalyser stage composed of nine analyzer crystals in the  $2\theta$  range  $0\text{-}33^\circ$ . The patterns were collected every  $10 \text{ }^\circ\text{C}$  below  $92 \text{ }^\circ\text{C}$  and in the  $122\text{-}152 \text{ }^\circ\text{C}$   $T$ -range and every  $5 \text{ }^\circ\text{C}$  between  $92 \text{ }^\circ\text{C}$  and  $122 \text{ }^\circ\text{C}$  in order to obtain the best resolution in the  $T$  range critical for the dehydration process. Between  $152$  and  $550 \text{ }^\circ\text{C}$  the patterns were recorded every  $50 \text{ }^\circ\text{C}$ , while above  $550$  every  $100 \text{ }^\circ\text{C}$ . Selected patterns are reported in Figure 1S.

### 3.4 Structural refinements

The GSAS package [22] with EXPGUI interface [23] was used for Rietveld profile fitting. Structure refinements were performed in the  $P6cc$  space group, starting from the framework atomic coordinates of [14]. The water molecule positions were determined by inspecting the Fourier difference maps. No evidence of thermal-induced symmetry change was found from the analysis of the powder patterns (Figure 1S).

The Bragg-peak profiles were modeled by a pseudo-Voigt function proposed by [24] with a peak intensity cut-off set to  $0.001$  of the peak maximum. The background curve was fitted with a Chebyshev polynomial with 18 coefficients. The overall scale factor, the  $2\theta$ -zero shift and the unit cell parameters were accurately refined for each histogram over the whole temperature range. Soft constraints were imposed on the tetrahedral bond lengths Al-O ( $1.68 \text{ \AA}$ ) and P-O ( $1.57 \text{ \AA}$ ), with a tolerance value of  $0.03$ . The isotropic thermal displacement parameters were constrained in order to have the same value for all the framework oxygen atoms, another for the tetrahedral cations, and a third for the water oxygen atoms. The refined structural parameters for each histogram were as follows: fractional coordinates and isotropic displacement factors for all atoms, and occupancy factor only for the extraframework species.

$\text{AlPO}_4\text{-}5$  unit cell parameters up to  $850 \text{ }^\circ\text{C}$  are reported as Supplementary Materials in Table 1S. The final observed and calculated powder patterns at  $rT$ ,  $82 \text{ }^\circ\text{C}$  and  $152 \text{ }^\circ\text{C}$  are shown in Figure 2S. For the same selected temperatures, lattice parameters and refinement details are reported in

Table 1, the atomic coordinates are reported in Table 2S. Tetrahedral cations and water molecule bond distances are reported in Table 3S.

## 4. Results and Discussion

### 4.1 Thermogravimetric analysis

Figure 3 shows the results of the two TG and DTG analyses performed on the calcined  $\text{AlPO}_4\text{-5}$  sample. In TG1, performed few days after calcination, the weight loss is 7.7% and corresponds to 7.6 water molecules per unit cell (p.u.c.); it occurs mostly below 100° C range with the DTG maximum at 57 °C. In TG2, performed several months after, the weight loss occurs mostly below 130° C range and corresponds to 16.5 water molecules p.u.c. (about 16.8 wt.%). The maximum of the DTG curve is at 86 °C. The different weight loss in the two experiments indicates that the water re-adsorbed in  $\text{AlPO}_4\text{-5}$  sample largely varies depending on the time passed from calcination and on the environment humidity.

### 4.2 Structural refinements

#### 4.2.1 Cell parameters

$\text{AlPO}_4\text{-5}$  maintains a good crystallinity up to the highest investigated temperature (Figure 1S). This is in agreement with its rehydration ability, proved by the two thermogravimetric analyses collected at different times after calcination. A good rehydration efficiency is taken as an indication of a preserved good crystallinity, and hence of the high thermal stability of the heated zeolite. Cruciani [25] introduced the parameter Stability Index (SI) to quantify the thermal stability of zeolites, based on the zeolite breakdown temperature determined by X-ray diffraction studies. The SI parameter for  $\text{AlPO}_4\text{-5}$  is the highest observed, namely 5, with the collapse temperature  $T_{\text{coll}} > 800$  °C. The cell parameter variations here reported suggest that  $\text{AlPO}_4\text{-5}$  framework is essentially rigid over the whole  $T$ -range analyzed (Table 1S).

The variations of  $a$  and  $c$  parameters in the whole investigated  $T$ -range are very small (+0.38 and +0.076, respectively, from  $rT$  to 850 °. The maximum expansion of the unit cell volume occurs at 152 °C corresponding to an increase of about 1.35% from  $rT$  (Figure 4a). Above this temperature, the cell volume decreases up to the final investigated  $T$ , evidencing a Negative Thermal Expansion (NTE) behavior, with  $\Delta a = -0.17\%$ ,  $\Delta c = -0.16\%$ , and  $\Delta V = -0.50\%$  (Figure 4a).

Our high-resolution study revealed a worth noting discontinuous trend below 150 °C, as a function of temperature (Figure b). After an initial slight increase of both  $a$  and  $c$  parameters between  $rT$  and 62 °C, in the range 62-82 °C  $a$  shows a marked further increase, while  $c$  decreases.

Then, above 82 °C and up to 97°C, there is an inversion in the behavior of cell parameters. Finally, above 97 °C, *c* remains almost constant while *a* increases further up to 152 °C.

#### 4.2.2 Water release and framework structural deformations

In the structural refinement at *rT*, 13.13 water molecules p.u.c. were found distributed over 6 partially occupied extra-framework sites (Table 2S, Figure 5). Five of them (W2, W3, W4, W5, W6) are located in the 12MR channel and one (W1) in the 6MR “pseudo-cage”. Four of these water molecules (W1, W2, W3, W5) are H-bonded with framework oxygen atoms, with minimum distances of 2.56 Å (Table 3S), while W4 and W6 only interacts with other water molecules. The water content estimated from the refinement (13.13 molecules p.u.c.) is intermediate between those found from TG1 (7.6) and TG2 (16.5), indicating a further different degree of hydration of the sample at the time of the XRPD measurement.

At 152 °C the sample is almost completely dehydrated. In fact, at this temperature, the Fourier maps of electronic density differences allowed to locate only one weak peak - corresponding to site W5 and accounting for 0.74 water molecules. This is in accordance with what found by TG analyses, showing that the water is released below 130°C. The slight difference in temperature could be due to the different sample environment during heating (i.e. a packed capillary for XRPD analyses and an opened crucible for TGA).

Figure 6, reporting the variation of the total water content calculated from the refinements, shows that dehydration occurs mainly in the *T* range 90-120 °C. The water loss determined by the structural refinement between 72 °C and 77 °C is due to the removal of W2 molecule (Figure 6). In fact, at 72°C W2 - O2 bond distance begins to be unrealistic, suggesting a shortcoming involving this site. As reported in literature [4,26,18], even at *rT*, O2 oxygen atom has a large anisotropic displacement parameter, characterized by a disk shape, located on the plane perpendicular to [001], where W2 is also confined. Hence it is very difficult to separate the contributions of O2 and W2 to the electronic density. For this reason, at 72 °C W2 was removed from the refinement. The removal of the W2 site is accompanied by an increase of W3 occupancy factor (Table S2 and Figure 6).

Water site W1 – located in the 6MR “pseudo-cage”– completely disappears between 82 and 92 °C, accompanied by the contemporary increase of W6 occupancy in the 12MR channel (Figure 6). This indicates that the water release is preceded by a water migration: W1 moves from the 6MR “pseudo-cage” to the main channel, through the hexagonal window that connects the “pseudo-cage” to the 12MR channel (Figure 5 and 7). This mechanism is confirmed by the “breathing” of the 6MR between 62 and 97 C. Specifically, the mentioned ring opens along the O1-O4 diameters leading to

the observed increase of the  $a$  parameter. A direct consequence of this phenomenon is the shortening of the Al-P distance, resulting in the  $c$  parameter reduction.

During dehydration, in the  $T$ -range 62-92 °C, structural modifications involves the 12MR channel as well. In fact, both O1-O1 and O3-O3 diameters increase during water release (Figure 8). The dehydration is accompanied by a significant opening of Al-O1-P bond angle, leading to a more circular channel and thus favoring the diffusion of the water molecules. On the contrary, Al-O3-P angle, shared by the 12MR and the 4-membered ring, appears less involved in the deformation. This is probably a consequence of the larger stiffness of 4-rings with respect to that of 6MR ones. Anyway, slight deformations, deriving from the modifications of 12MR and 6MR, are observed even for the 4-ring. Specifically, during dehydration, its diameters O3-O3 and O4-O4 change following opposite trends (decreasing and increasing, respectively, Figure 3S), so conferring a more regular square-shape to the 4-ring.

#### 4.2.4 Negative Thermal Expansion

Negative Thermal Expansion, defined as a reversible contraction of the unit cell upon heating, has been identified in a wide range of compounds, including the dehydrated forms of several zeolites (and zeotypes). Cruciani [25], in his review of the thermal behavior of zeolites, states that NTE is rare among natural zeolites (e.g. analcime [27]), whereas among synthetic zeolites it is more common, occurring in MFI (ZSM-5) [15,28], Na-X [29], zeolite A [30], FAU [31,32], RHO [33], MWW, ITE and STT [34], CHA and IFR [35,36], ISV and STF [37], FER [38], most of them being in their pure silica form. According to Sleight [39], NTE can be either isotropic or anisotropic, depending on whether the contraction occurs in all three directions, or only in one or two.

After complete dehydration above 152° C and up to 850° C,  $\text{AlPO}_4\text{-5}$  undergoes a barely perceptible NTE ( $\Delta V=-0.5\%$ ,  $\Delta a=-0.17\%$   $\Delta c=-0.15\%$ ). The corresponding thermal expansion coefficients are  $\alpha_v = -7.12 (10^{-6}/\text{K})$ ,  $\alpha_a = -2.5 (10^{-6}/\text{K})$ ,  $\alpha_c = -2.2 (10^{-6}/\text{K})$ , indicating an almost isotropic NTE behavior. These very tiny variations made impossible a detailed structural interpretation of the phenomenon.

The NTE behavior of  $\text{AlPO}_4\text{-5}$  in the  $T$  range 151-501° C was already discussed by [15]. The authors report the following expansion coefficients for their  $\text{AlPO}_4\text{-5}$  sample:  $\alpha_v = -14.5(10^{-6}/\text{K})$ ,  $\alpha_a = -5.1(10^{-6}/\text{K})$ ,  $\alpha_c = -3.7(10^{-6}/\text{K})$ . These coefficients are higher than those found in this work (even more if we consider the same  $T$ -range (i.e.:  $\alpha_v = -5.75(10^{-6}/\text{K})$ ,  $\alpha_a = -2.4(10^{-6}/\text{K})$ ,  $\alpha_c = -1.1(10^{-6}/\text{K})$ ). The differences found in the expansion coefficient values can be ascribed to the different experimental conditions adopted in the two experiments: Park et al. [15] worked with a Lenné-

Guinier camera using an extremely slow heating rate ( $5^{\circ}$  C/h), while in the present study the temperature was increased at a rate of  $5^{\circ}$ /min. A further possible consequence of the extended thermal treatment applied by Park et al. was the appearance of a tridymite-type phase between 502 and 647  $^{\circ}$ C, which was not observed in the present study.

Leardini et al. [32] recently reviewed the NTE behavior of a large number of dehydrated zeolites. Comparing the expansion coefficients of  $\text{AlPO}_4\text{-5}$  to those reported in Table 4 by Leardini et al., it can be seen that, over the wide  $T$  range 150-850 $^{\circ}$  C,  $\text{AlPO}_4\text{-5}$  is one of the most rigid frameworks studied to date, including the other aluminophosphate materials investigated.

It is also interesting to compare the thermal behavior of  $\text{AlPO}_4\text{-5}$  with that of zeolite L [40], another zeolite widely used as host matrix for dye molecules and characterized by the presence of a mono-dimensional 12MR channel system. Zeolite L completely dehydrates at very low  $T$  (about 230 $^{\circ}$  C), has a very high thermal stability, maintains good crystallinity at least up to 814  $^{\circ}$ C, and is essentially rigid, with the total variations of the  $a$ ,  $c$ , and  $V$  parameters 0.2%, 0.3% and 0.7%, respectively. However, zeolite L does not undergo NTE.

## 5. Conclusions

The thermal stability and  $T$ -dependence of the unit cell parameters and crystal structure of  $\text{AlPO}_4\text{-5}$  were investigated by in situ synchrotron XRPD experiments performed from  $rT$  to 850  $^{\circ}$ C. No phase transitions were observed in the investigated  $T$  range. Dehydration is almost complete at 152  $^{\circ}$ C and occurs after water migration from small to large pores. During the water removal, the cell volume increases to facilitate the molecule release. Above 152 $^{\circ}$  C and up to 850  $^{\circ}$ C,  $\text{AlPO}_4\text{-5}$  undergoes a very weak NTE, as already noted by Park et al [**Error! Bookmark not defined.**]. However, as a whole,  $\text{AlPO}_4\text{-5}$  behaves as an essentially rigid framework. This can be explained on the basis of the very low interactions between framework and water molecules, even at room temperature.

## Acknowledgements

The European Synchrotron Radiation Facility is acknowledged for allocating beam time at the beamline ID22. This work was supported by the Italian MIUR (PRIN2015 Prot. 2015HK93L7; project title “ZAPPING. High-pressure nano-confinement in Zeolites: the Mineral Science know-how APPLIED to engineerING of innovative materials for technological and environmental applications”). The Editor and two anonymous referees are acknowledged for their comments, that strongly helped the authors in improving the manuscript.

## References

- 
- [1] S.T. Wilson, B.M. Lok, C.A. Messina, T.R. Cannan, E.M. Flanigen, *J. Am. Chem. Soc.* 104 (1982) 1146-1147.
- [2] E.M. Flanigen, B.M. Lok, R.L. Patton, S.T. Wilson, *Pure Appl. Chem.* 58 (1988) 1351-1358.
- [3] J. Yu, R. Xu, *Acc. Chem. Res.* 36 (2003) 481-490.
- [4] J.M. Bennet, J.P. Cohen, E.M. Flanigen, J.J. Pluth, J.V. Smith, in: G.D. Stucky, F.G. Dwyer (Eds.), *Intrazeolite Chemistry*, ACS Sym. Ser., 218, American Chemical Society, Washington DC, 1983, pp. 109-118.
- [5] C. Baerlocher, L.B. McCusker, D.H. Olson in: *Atlas of Zeolite Framework Types*, sixth ed., Elsevier, Amsterdam, 2007.
- [6] D. Liu, B. Zhang, X. Liu, J. Li, *Catal. Sci. Technol.* 5 (2015) 3394-3402.
- [7] Y. Chen, Y. Zhang, D. Li, F. Gao, C. Feng, S. Wen, S. Ruan, *Sensor. Actuat. BChem.* 212 (2015) 242-247.
- [8] W. Yang, W. Sun, S. Zhao, X. Yin, *Micropor. Mesopor. Mat.* 219 (2016) 87-92.
- [9] G. Calzaferri, *Langmuir* 28 (2012) 6216-6218.
- [10] G. Calzaferri, K. Lutkouskaya, *Photochem. Photobiol. Sci.* 7 (2008) 879-910.
- [11] G. Calzaferri, R. Méallet-Renault, D. Brühwiler, R. Pansu, I. Dolamic, T. Dienel, P. Adler, H. Li, A. Kunzmann, *Chem. Phys. Chem.* 12 (2011) 580-594.
- [12] H. Lv, M. Yao, Q. Li, R. Liu, B. Liu, S. Lu, L. Jiang, W. Cui, Z. Liu, J. Liu, Z. Chen, B. Zou, T. Cui, B. Liu, *J. Appl. Phys.* 111 (2012) 112615-1-112615-5.
- [13] T. Kim, Y. Lee, Y-N. Jang, J. Shin, S.B. Hong, *Micropor. Mesopor. Mat.* 169 (2013) 42-46.
- [14] P. Lotti, G.D. Gatta, Comboni D. Merlini M., Pastero L., Hanfland M., *Micropor. Mesopor. Mat.* 228 (2016) 158-167.
- [15] S.H. Park, R.-W. Große Kunstleve, H. Graetsch, H. Gies, *Stud. Surf. Sci. Catal.* 105 (1996) 1989-1994.
- [16] P. Bordat, J. Kirstein, P. Labéguerie, M. Merawa, R. Brown, *J. Phys. Chem. C* 111 (2007) 10972-10981.
- [17] A.J. Mora, A.N. Fitch, M. Cole, R. Goyal, R.H. Jones, H. Jobic, S.W. Carr, *J. Mater. Chem.* 6 (1996) 1831-1835.
- [18] G.J. Klap, H. van Koningsveld, H. Graafsma, A.M. Shreurs, M., *Micropor. Mesopor. Mat.* 38 (2000) 403-412.
- [19] Y. Liu, R.L. Withers, L. Norén, *Solid State Sci.* 5 (2003) 427-434.
- [20] A. Berlie, G.J. Kearley, Y. Liu, D. Yu, R.A. Mole, C.D. Ling, R.L. Withers, *Phys. Chem. Chem. Phys.* 17 (2015) 21547-21554.
- [21] D. Liu, B. Zhang, X. Liu, J. Li, *Catal. Sci. Technol.* 5 (2015) 3394-3402.
- [22] A.C. Larson, R. B. Von Dreele, *General Structure Analysis System "GSAS"*; Los Alamos National Laboratory Report; Los Alamos, 1994; LAUR 86-748.
- [23] B.H. Toby, *J. Appl. Crystallogr.* 34 (2001) 210-213.
- [24] P. Thomson, D.E. Cox, J.B. Hastings, *J. Appl. Crystallogr.* 20 (1987) 79-83.
- [25] G. Cruciani, *J. Phys. Chem. Solids* 67 (2006) 1973-1994.
- [26] T. Ikeda, K. Miyazawa, F. Izumi, Q. Huang, A. Santoro, *Phys. Chem. Solids* 60 (1999) 1531-1535.
- [27] G. Cruciani, A. Gualtieri, *Am. Mineral.* 84 (1999) 112-119.
- [28] P.M. Jardim, B.A. Marinkovic, A. Saavedra, L.Y. Lau, C. Baehtz, F. Rizzo, , *Microporous Mesoporous Mater.* 76 (2004) 23-28.
- [29] J.W. Couves, R.H. Jones, S.C. Parker, P. Tschaufeser, C.R.A. Catlow, *J. Phys. Condens. Matter* 5 (1993) 329-332.



- 
- [30] A. Colantuono, S. dal Vecchio, G. Mascolo, M. Pansini, *Thermochim. Acta* 296 (1997) 59–66.
- [31] M.P. Attfield, A.W. Sleight, *Chem. Commun.* (1998) 6001–6602.
- [32] L. Leardini, S. Quartieri, G. Vezzalini, R. Arletti, *Micropor. Mesopor. Mat.* 202 (2015) 226–233
- [33] A. Bieniok, K.D. Hammonds, *Micropor. Mesopor. Mat.* 25 (1998) 193–200.
- [34] D.A. Woodcock, P. Lightfoot, P.A. Wright, L.A. Villaescusa, M.J. Diaz-Cabanas, M.A. Cambor, *J. Mater. Chem.* 9 (1999) 349–351.
- [35] L.A. Villaescusa, P. Lightfoot, S.J. Teat, R.E. Morris, *J. Am. Chem. Soc.* 123 (2001) 5453–5459.
- [36] D.A. Woodcock, P. Lightfoot, P.A. Wright, L.A. Villaescusa, M.J. Diaz-Cabanas, M.A. Cambor, D. Engberg, *Chem. Mater.* 11 (1999) 2508–2514.
- [37] P. Lightfoot, D.A. Woodcock, M.J. Maple, L.A. Villaescusa, P.A. Wright, *J. Mater. Chem.* 11 (2001) 213–225.
- [38] I. Bull, P. Lightfoot, L.A. Villaescusa, L.M. Bull, R.K. Gover, J.S. Evans, R.E. Morris, *J. Am. Chem. Soc.* 125 (2003) 4342–4349.
- [39] A.W. Sleight, *Curr. Opin. Solid State Mater. Sci.* 3 (1998) 128–131.
- [40] L. Gigli, R. Arletti, S. Quartieri, F. Di Renzo, G. Vezzalini, *Micropor. Mesopor. Mat.* 177 (2013) 8–16

Figure 1  
[Click here to download high resolution image](#)

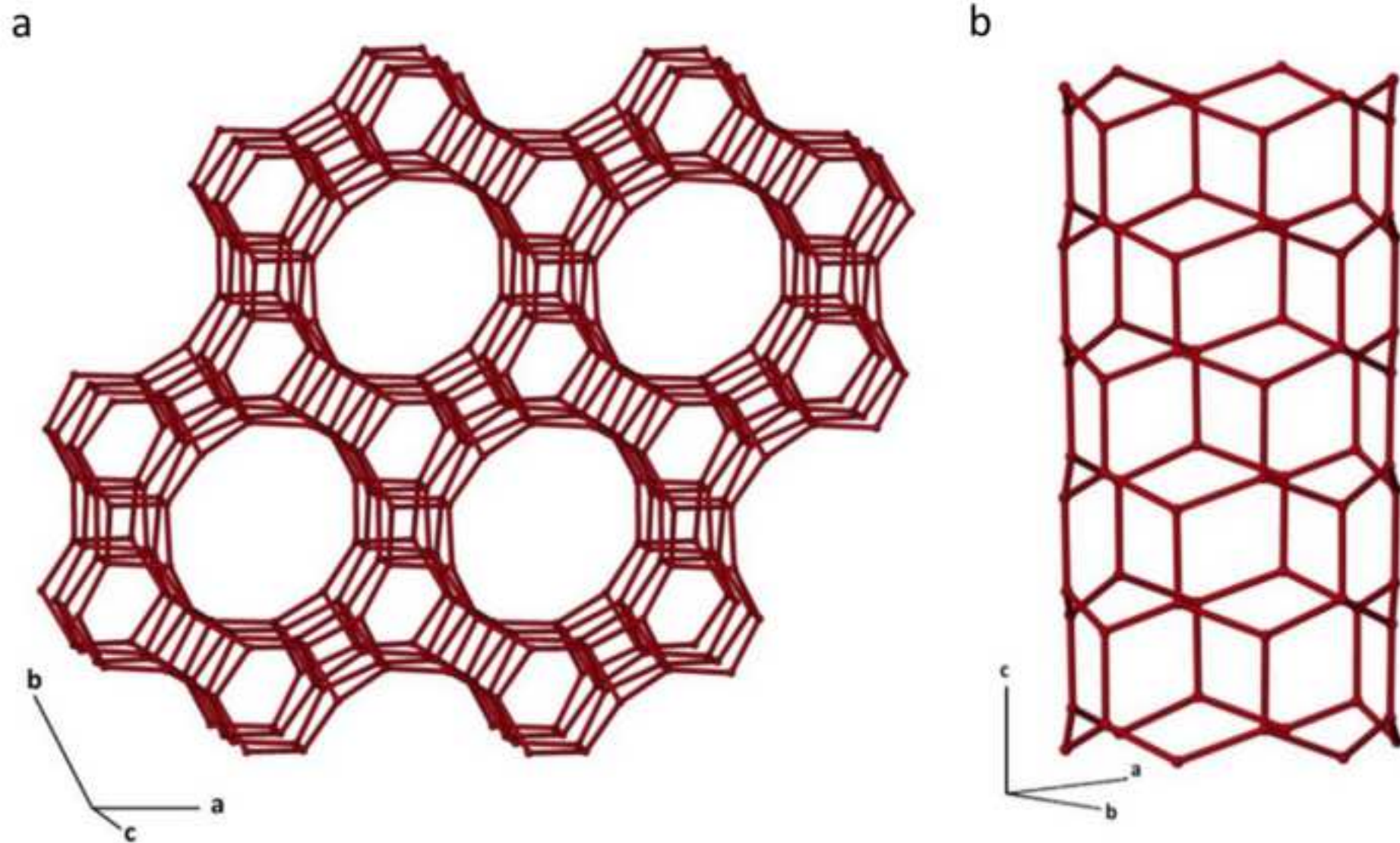


Figure 2  
[Click here to download high resolution image](#)

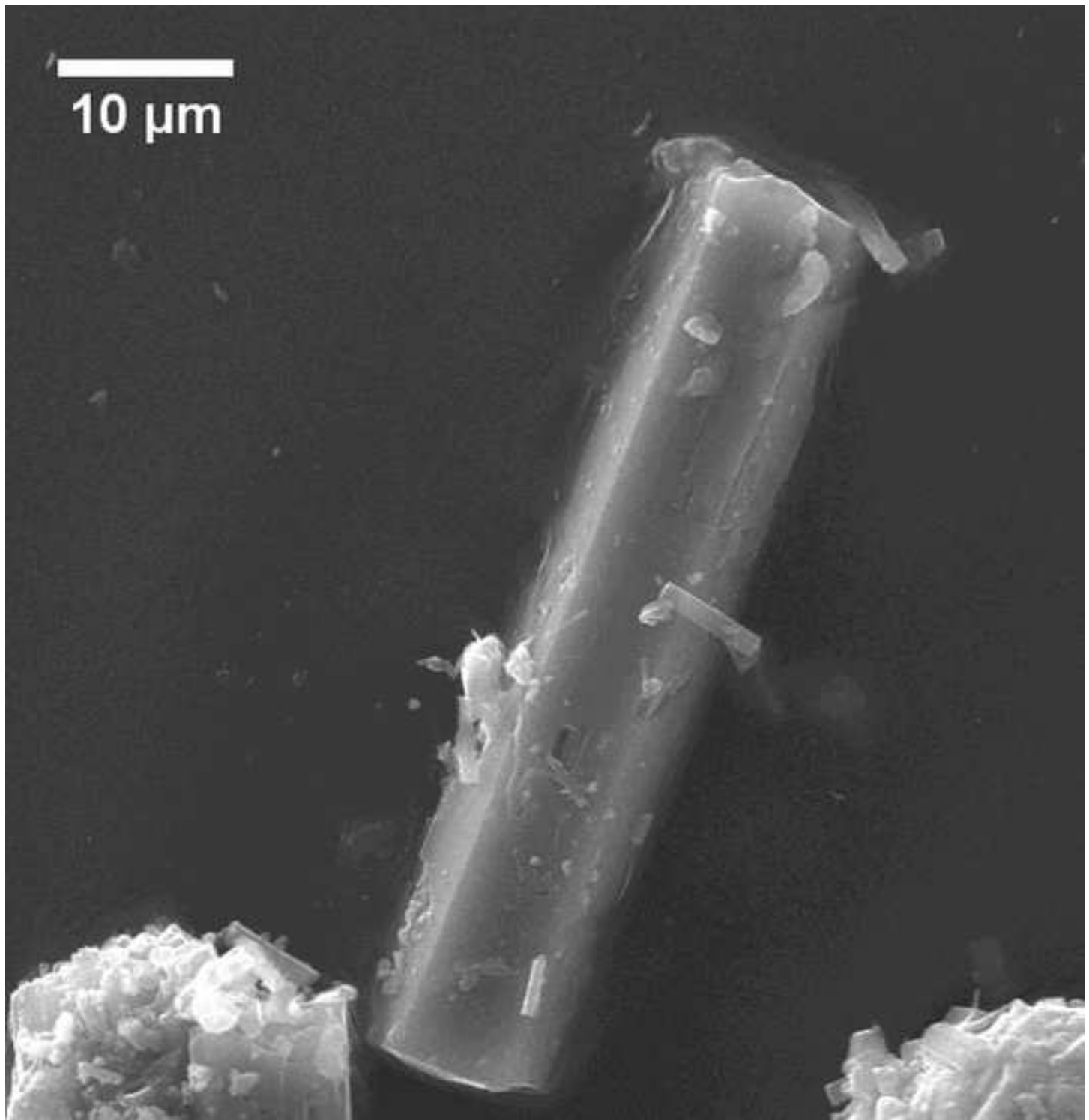


Figure 3a  
[Click here to download high resolution image](#)

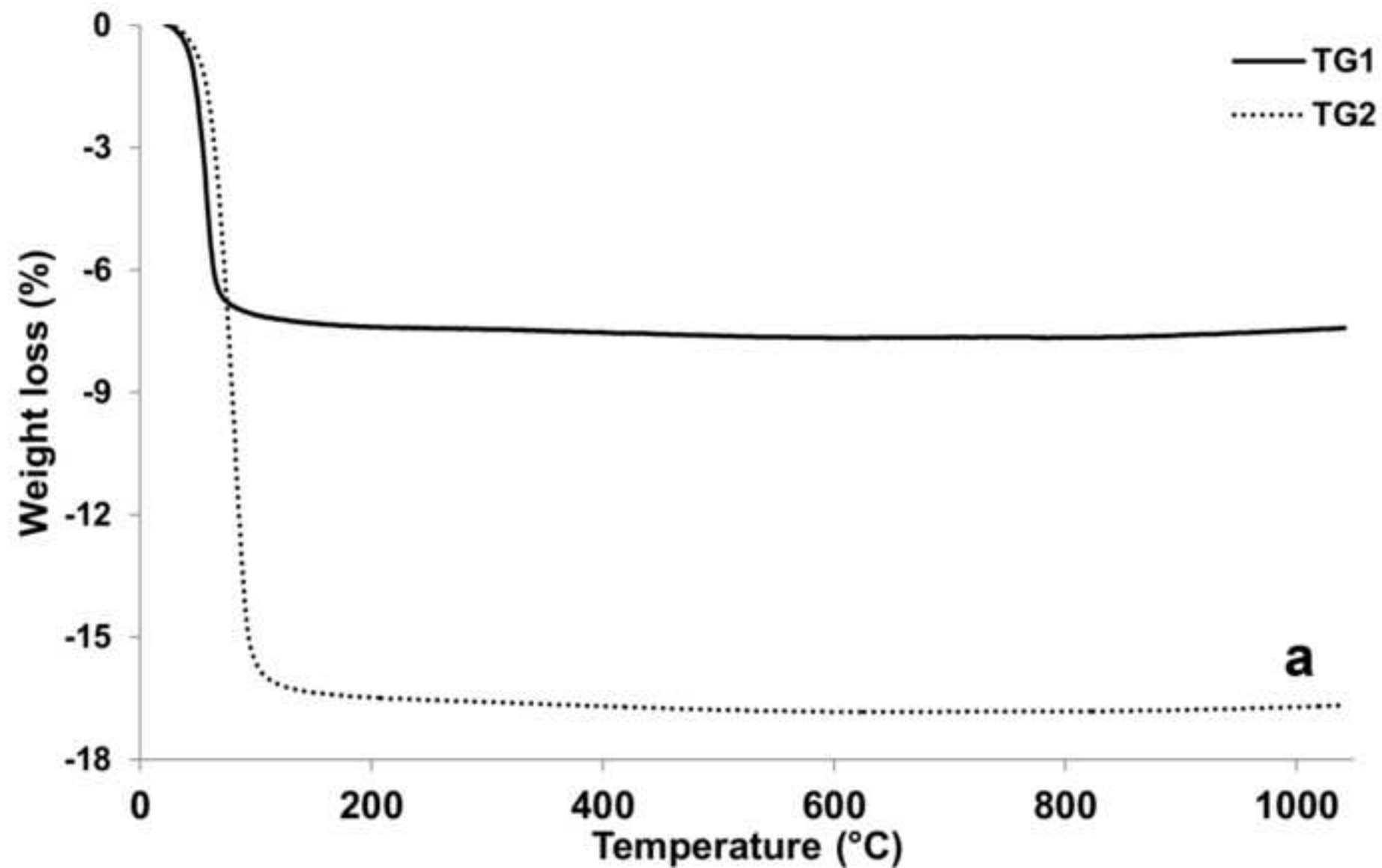


Figure 3b  
[Click here to download high resolution image](#)

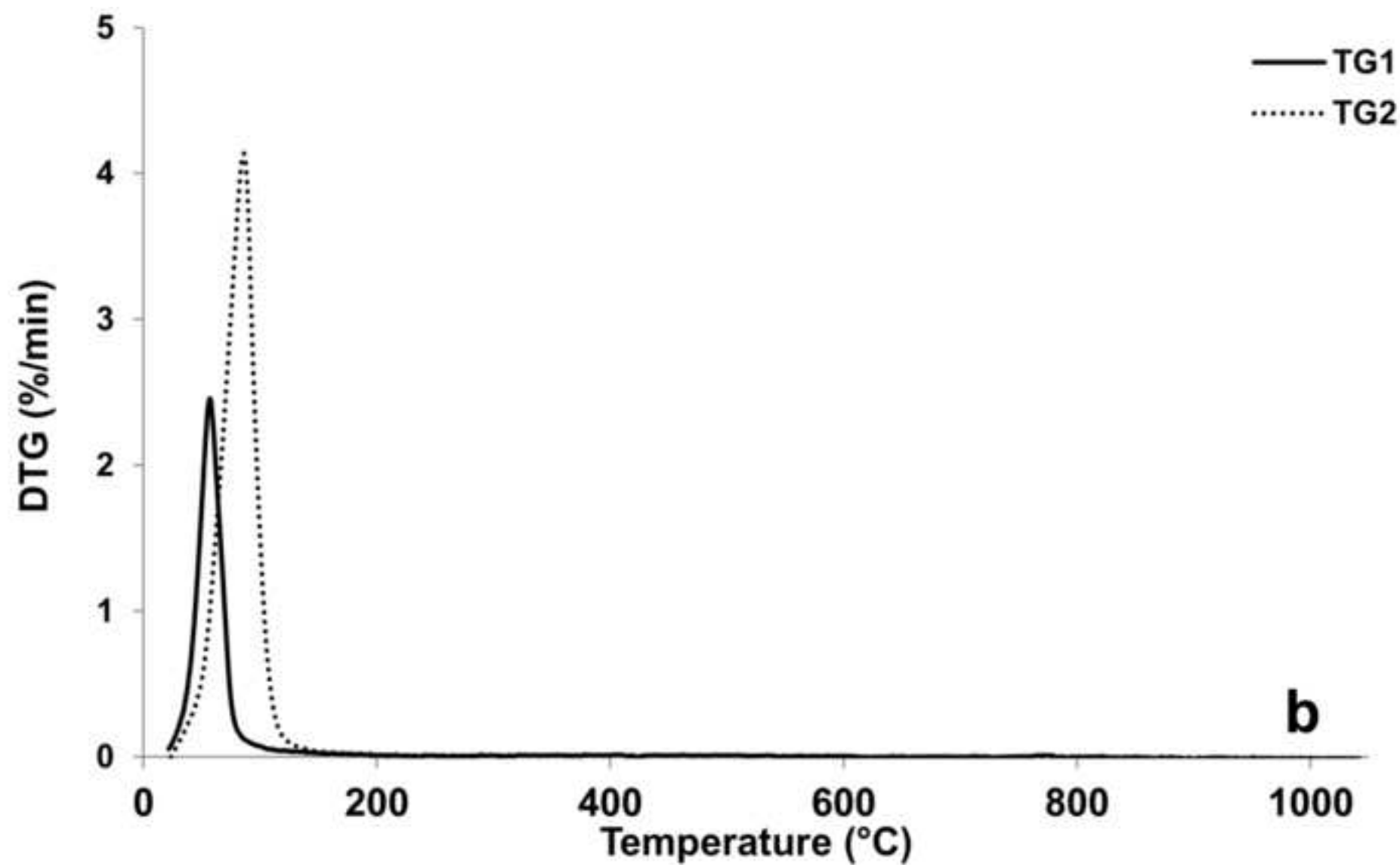


Figure 4a  
[Click here to download high resolution image](#)

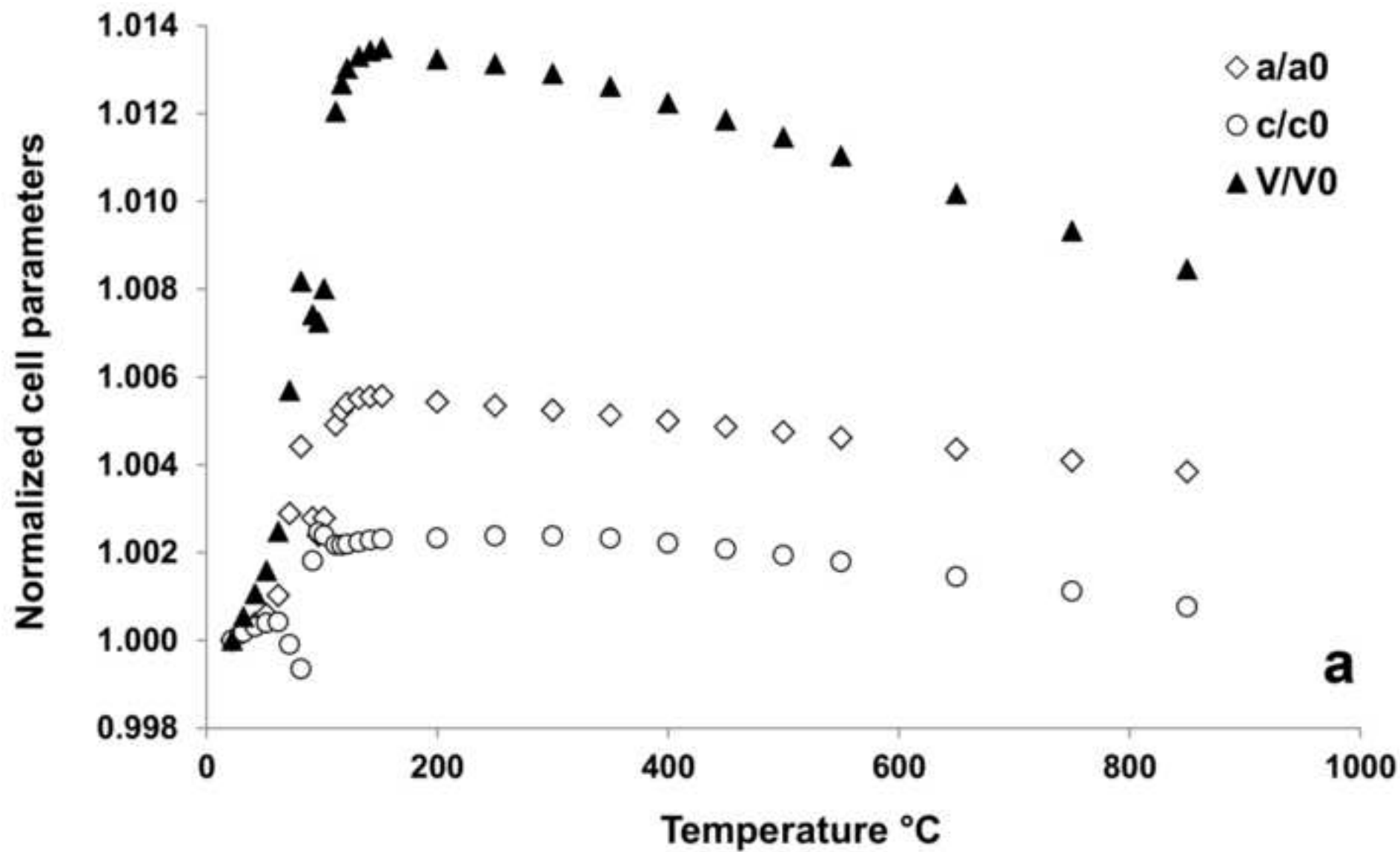
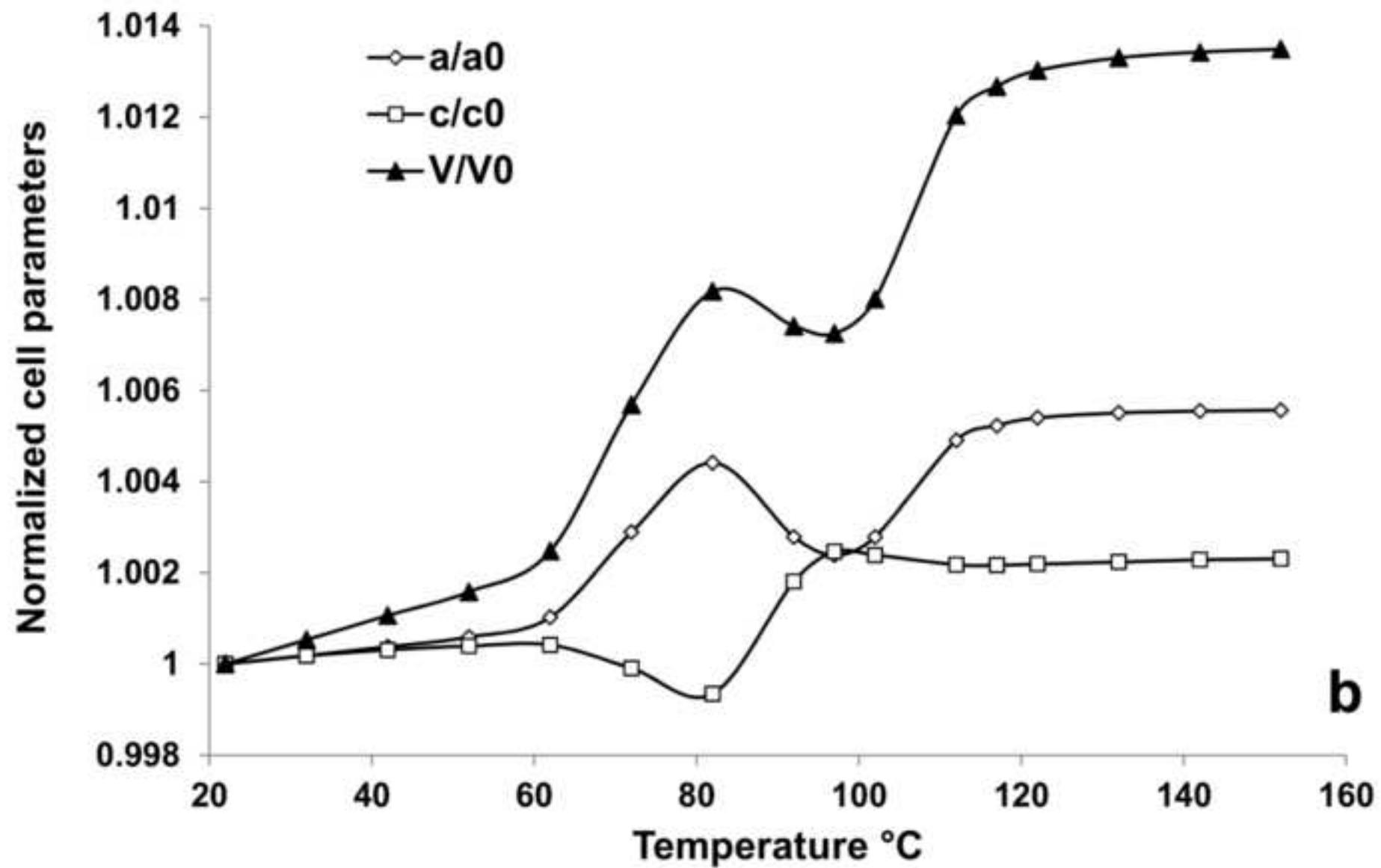


Figure 4b  
[Click here to download high resolution image](#)



**b**

Figure 5  
[Click here to download high resolution image](#)

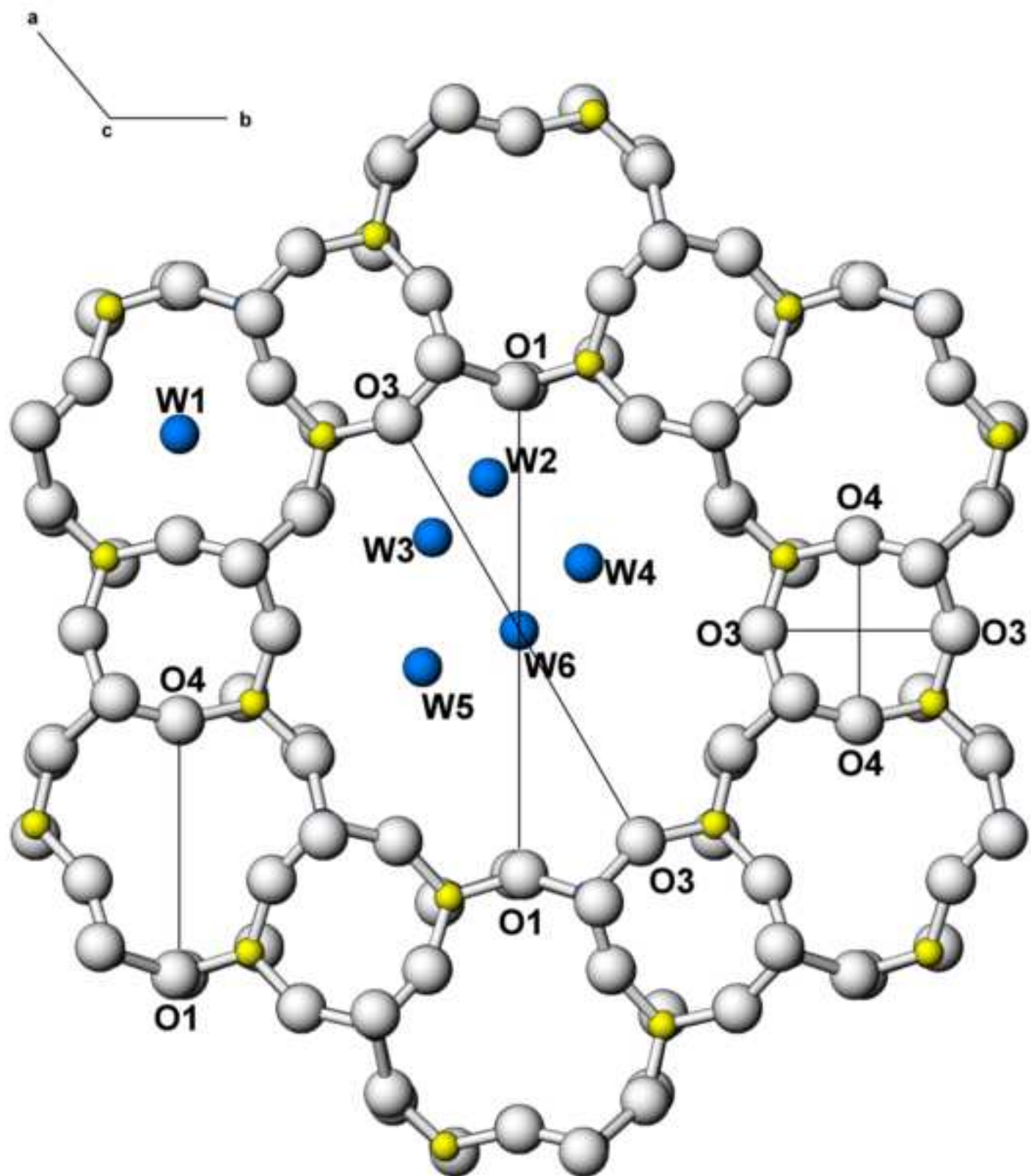




Figure 6  
[Click here to download high resolution image](#)

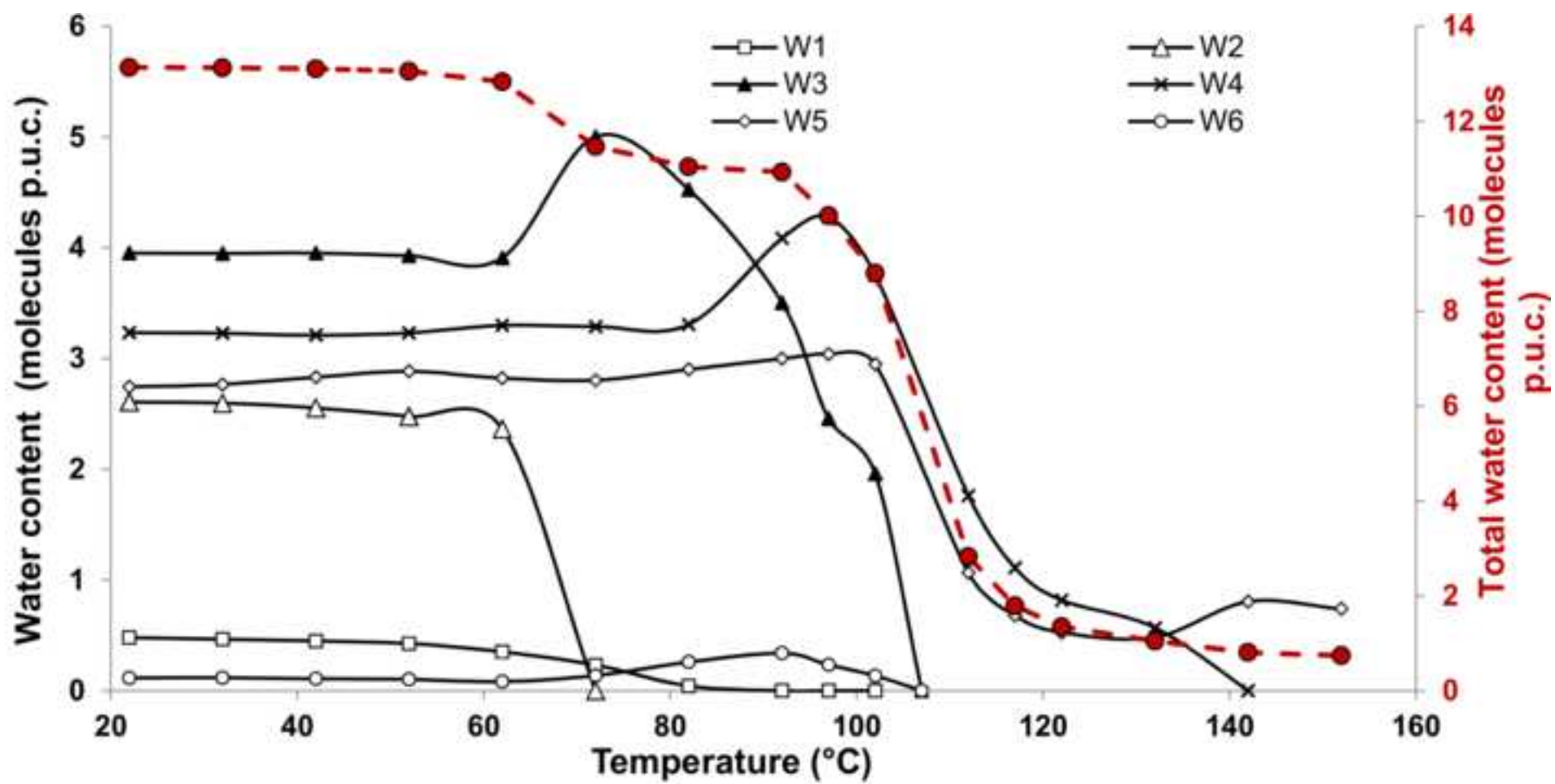


Figure 7  
[Click here to download high resolution image](#)

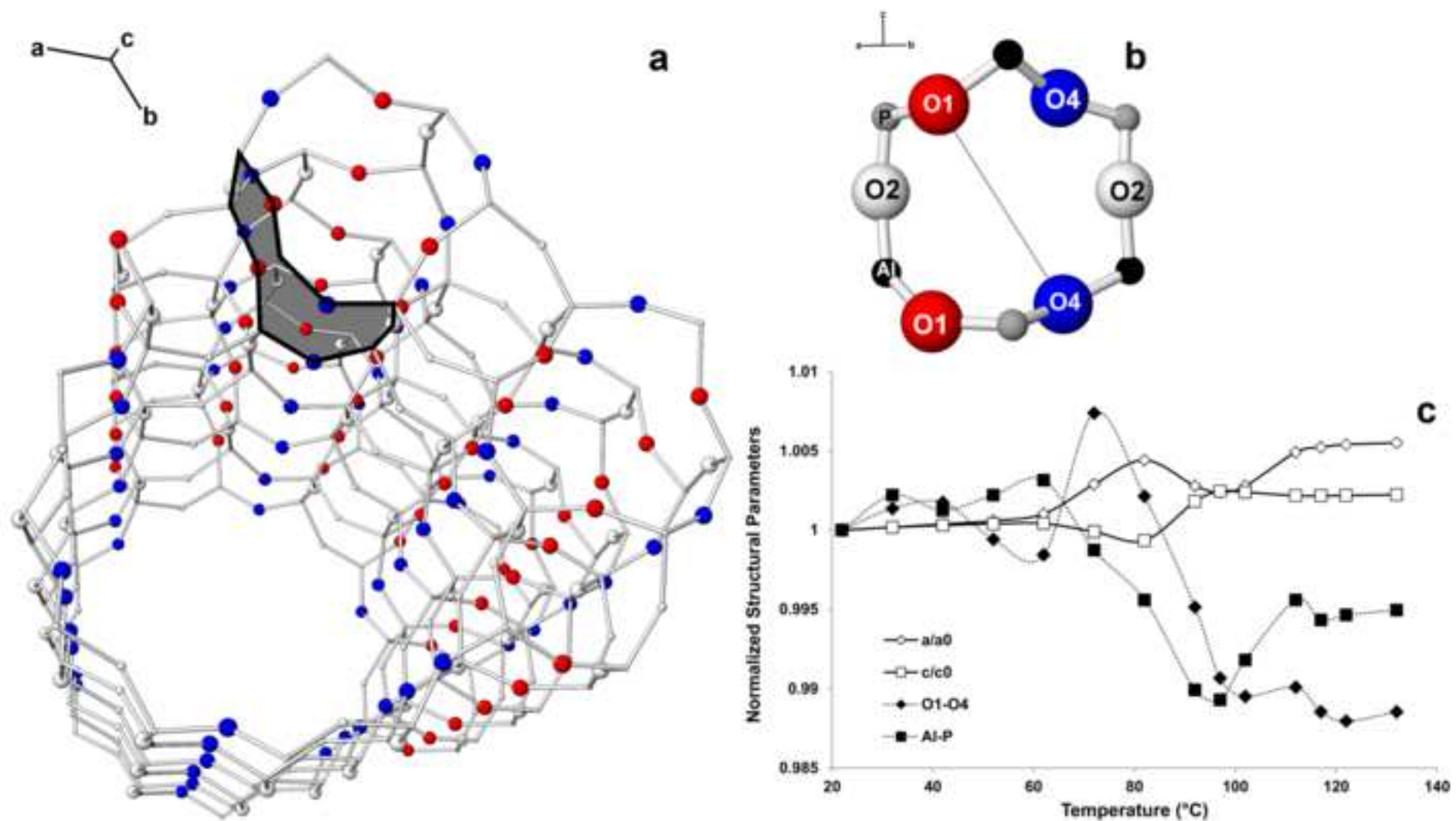
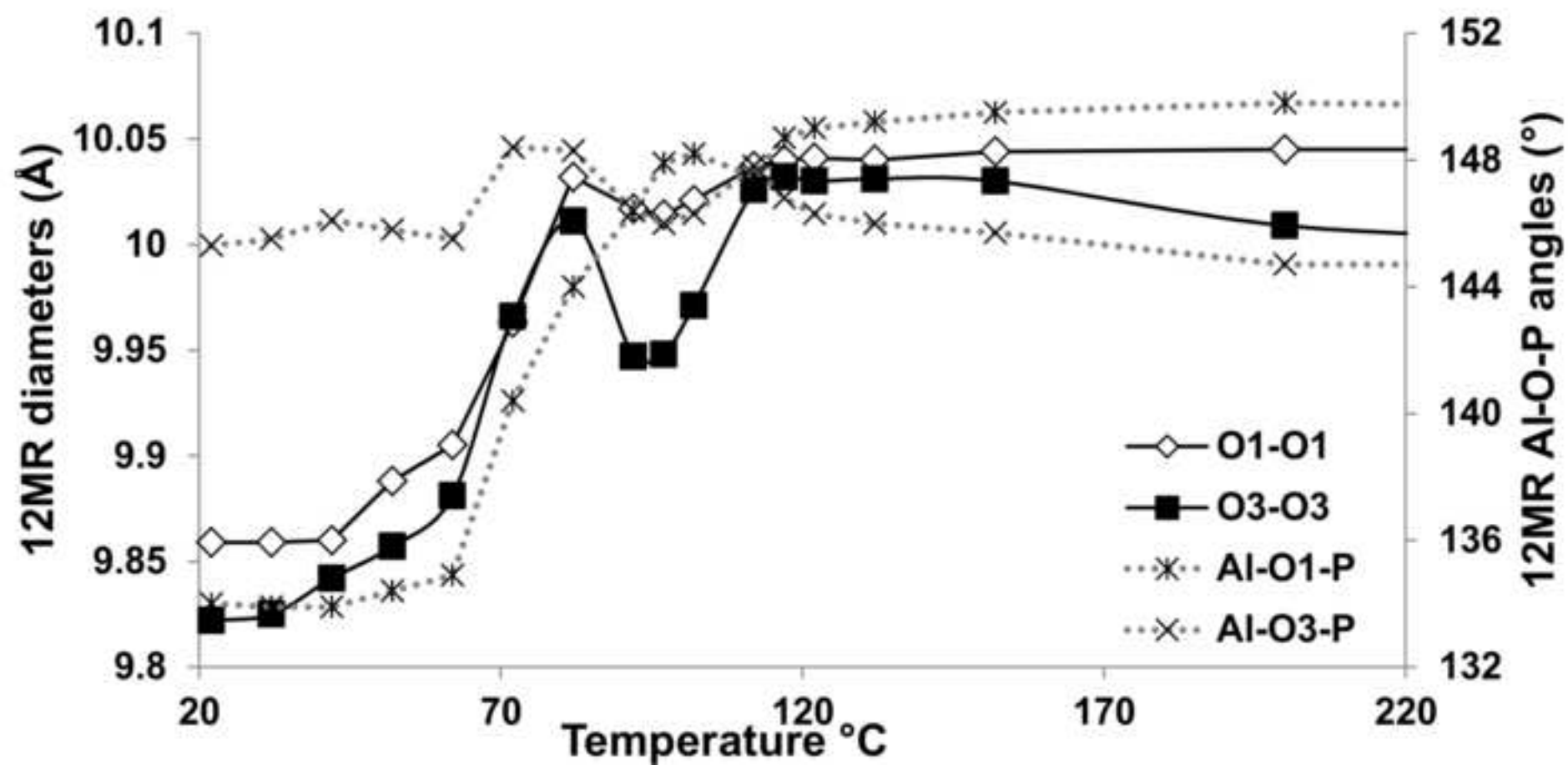


Figure 8  
[Click here to download high resolution image](#)



**Supplementary Material**

[Click here to download Supplementary Material: S1rev.docx](#)